Journal of Solid State Chemistry **155,** 389–393 (2000)
doi:10.1006/jssc.2000.8929, available online at http://www.idealibrary.com on IDEAL®

Synthesis and Neutron Diffraction Study of $La_5Si_2BO_{13}$, an Analog of the Apatite Mineral

D. Mazza,* M. Tribaudino,† A. Delmastro,* and B. Lebech‡

*Dipartimento di Scienza dei Materiali e Ingegneria Chimica, Politecnico di Torino, C.so Duca degli Abruzzi 24, I-10129 Torino, Italy;
†Dipartimento di Scienze Mineralogiche e Petrologiche, Università di Torino, Via V.Caluso, I-10100 Torino, Italy;
‡Risø National Laboratory, FYS-108, DK-4000 Roskilde, Denmark

Published online November 29, 2000

The structure refinement of an apatite homolog, $La_5Si_2BO_{13}$, was performed from neutron powder diffraction spectra. The refined sample was synthesized from gel during an investigation of apatite-like compounds with the general formula $La_{9.33+x}Si_{6-3y}B_{3y}O_{26}$ (space group, $P6_3/m$; $Z = 2$) in an electric furnace at $T = 1100°C$ for 3 h. Two spectra, collected at $\lambda = 1.558$ and 2.439 Å at Risø National Laboratory (Denmark), were processed together for a Rietveld structure refinement ($wRp_{all} = 0.087$, $Rp_{all} = 0.067$, $\chi^2 = 2.2$; $a_0 = 9.5587(2)$; $c_0 = 7.2173(2)$ Å). Comparison with other apatite-like structures shows lower distortion in the $M1$ polyhedron and unusually short bond length from La in the $M2$ site and O4 oxygen in the column site (2.303 Å). These results can be explained in view of the presence of trivalent La and divalent O, respectively, in the $M1$, $M2$ sites and in the column anion site, whereas in apatites these sites are occupied by divalent and monovalent ions respectively.

Key Words: **neutron powder diffraction; Rietveld refinement; apatites; $La_5Si_2BO_{13}$.**

INTRODUCTION

In a previous study (1), the ternary phase diagram Al_2O_3–SiO_2–La_2O_3 showed that the binary oxide $La_{14}Si_9O_{39}$ extends its stability range inside the phase diagram by reason of a substitution of Al for Si. The solid solution can be expressed by the notation $La_{9.33+x}Si_{6-3x}Al_{3x}O_{26}$ (composition is referred to unit cell content), with $x = 0$ and $x = 0.33$; a typical apatite-like XRD pattern is found for all other compositions. In this structure, La is located in two independent positions, namely, La1 and La2, with multiplicity 6 and 4, respectively, with partial occupancy of La2.

This work is concerned with an apatite within the analogous homogeneity range encountered in the B_2O_3–SiO_2–La_2O_3 ternary system currently under investigation. In this case the wider homogeneity range is expressed by $La_{9.33+x}Si_{6-3x}B_{3x}O_{26}$ and extends from $x = 0$ to $x = 0.67$; at the limiting compositions $x = 0.67$, La2 is fully occupied, and the formula referred to unit cell is $La_{10}Si_4B_2O_{26}$ or, more simply, $La_5Si_2BO_{13}$ (Fig. 1).

Technological interest in this class of compounds has recently been aroused due to the high ionic oxygen conductivity reported for the compositions $RE_{10}Si_6O_{27}$ (RE = La, Pr, Nd, Sm, Gd, Dy). These ceramic oxides have been shown (2) to have apatite as a prevalent phase.

The composition $La_5Si_2BO_{13}$ is distinct among apatites because it is the only member of the apatite family that has the nontetrahedral cation sites (Ca1 and Ca2 in the $Ca_5(PO_4)OH$ reference structure) fully occupied by a trivalent cation (La^{3+}); Si and B are disordered in the tetrahedral site and the overall charge balance is maintained by the unusual presence of oxygen in the column site. It is therefore of interest to clarify the effect of the above substitution on the structural configuration.

The results of the refinement of the apatite-like structure $La_5Si_2BO_{13}$ are reported hereafter; the observed polyhedral configurations are also discussed as compared to other apatite-like structures.

EXPERIMENTAL

Preparation of the Samples

The compounds were obtained by a wet chemical procedure. Starting materials were $La(NO_3)_3 \cdot 6H_2O$ (Fluka, 99.9% purity), H_3BO_3 (Fluka, 99.9% purity), tetraethylorthosilicate (TEOS, Aldrich), and glycerol. A measured volume of TEOS is added to an equal volume of ethanol (95%) and a half volume of distilled water. The pH of the aqueous alcoholic phase is adjusted to $0.5 \sim 1.0$ with a few drops of HNO_3. In this way a clear solution is quickly obtained after some minutes of stirring at room temperature. The r factor (i.e., water moles/TEOS moles) reaches a value of about 7.

Under these conditions TEOS is first partially hydrolyzed to soluble silanol monomers. An aqueous solution of La nitrate and boric acid in stoichiometric amount is

0022-4596/00 $35.00

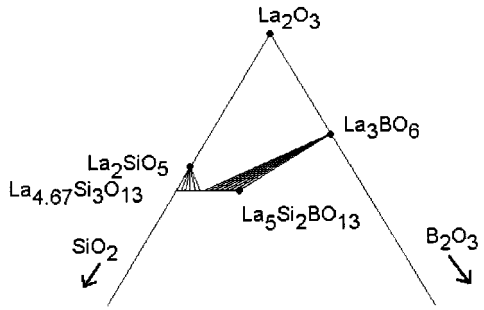

FIG. 1. Upper section of the ternary phase diagram La_2O_3–SiO_2–B_2O_3 at 1100°C.

then added to the proper quantity of the TEOS solution, together with some drops of glycerol. Glycerol is used as a reducing agent; it reacts in fact with boric acid to form ester complexes at room temperature, thereby improving boric acid solubility. The clear solution thus obtained is then treated with excess aqueous ammonia (30 wt%). Condensation and crosslinking of silanol monomers occurs rapidly, while lanthanum hydroxide precipitates. The obtained gel is first dried at 105°C and then gradually heated up to 500°C, in order to remove water and gaseous products formed by the decomposition of the nitrates and TEOS. The solids obtained by this procedure are normally found to be amorphous when examined by X-ray diffraction. They are thoroughly ground in an agate planetary mixer, pressed in tablets (3 kbar), and finally placed in an electric furnace and heated in air at 1100°C for 3 h. At this temperature B_2O_3 has a negligible vapor pressure and therefore the initial composition is preserved. Thermogravimetric measurements demonstrate indeed that no weigh loss is detectable up to 1200°C.

X-ray Powder Diffraction

Three samples of $La_{9.33+x}Si_{6-3x}B_{3x}O_{26}$ stoichiometry were prepared with $x = 0$, $x = 0.33$ and $x = 0.66$. The resulting white fine powders were monophasic when examined by X-ray diffraction (XRD). The sharp XRD peaks (not shown) were all indexable on the basis of a hexagonal cell. The dimensions are listed in Table 1. Other La-richer compositions were prepared to confirm the mixed crystals' stoichiometry. These off-stoichiometry samples resulted in biphasic products and the extra phases evidenced by X-ray diffraction (La_2SiO_5 and La_3BO_6) confirmed the compositional range and allowed us to trace part of the isothermal section of the phase diagram at 1100°C (as shown in Fig. 1).

Neutron Diffraction

In $La_5Si_2BO_{13}$ the presence of a strong scatterer like La affects the refinement of the lighter atoms when an X-ray source is used. It was therefore decided to perform the data collection with a neutron source. A ^{11}B-enriched sample was synthesized to overcome absorption problems caused by the presence of ^{10}B isotope, starting from 99% enriched H_3BO_3 (Sigma–Aldrich Corp.).

TABLE 1
Unit-cell Dimensions of the Samples in the Homogeneity Range

Composition	x value	a_0 (Å)	C_0 (Å)
$La_{9.33}Si_6O_{26}$	0	9.719[a]	7.183[a]
$La_{9.66}Si_5BO_{26}$	0.33	9.630	7.196
$La_{10}Si_4B_2O_{26}$	0.67	9.5587(2)[b]	7.2171(2)[b]

Note. Composition is referred to unit cell.
[a] From Ref. (3).
[b] Values obtained by neutron diffraction.

Neutron diffraction was carried out at the TAS3/POW large-scale facility in Risø National Laboratory (Denmark). Two constant wavelengths of $\lambda = 1.558$ and 2.439 Å were employed in a two-axis diffractometer setting and $\theta - 2\theta$ scan. The instrument was equipped with a pyrolytic graphite (002) monochromator and 20 ^3He simultaneous detectors. The spectra were both measured from 2θ 10° to 115°, corresponding to a maximum resolution of 0.92 and 1.44 Å.

Rietveld analysis was done to perform the structure refinement of $La_5Si_2BO_{13}$. Data histograms were processed by means of the GSAS package (3). The two profiles collected at different wavelengths were processed simultaneously. Synthetic $La_{4.67}Si_2O_{13}$ (4) was used as the starting structure, with $P6_3/m$ space group, assumed by similarity. A fully Gaussian profile function was used to fit the experimental patterns. The scale factor, the background, modeled with a Chebyshev polynomial with seven coefficients, and the lattice parameters were first refined, subsequently releasing the peak profile parameters, the coordinates, and the isotropic displacement parameters. The agreement factors were wRp = 0.078, Rp = 0.061, and $R(|F|^2) = 0.054$ for the spectrum collected at $\lambda = 1.558$ and wRp = 0.112, Rp = 0.090, and $R(|F|^2) = 0.099$ for the data collected at $\lambda = 2.439$ Å (Fig. 2).

The site occupancy for the tetrahedral site, where Si and B are present, was released in the final runs; no significant deviation from the expected stoichiometry was observed. Atomic parameters, isotropic and anisotropic displacement factors, and polyhedral bond lengths are reported in Tables 2, 3, and 4. The obtained structural configuration was verified by bond valence calculations (5); anomalous under or overbonding was not observed (Table 3).

RESULTS AND DISCUSSION

The structure of $La_5Si_2BO_{13}$ is discussed and compared with that of (Ca, Sr, Ba, Pb)$_5$(PO$_4$)$_3$(OH, Cl, F) apatites

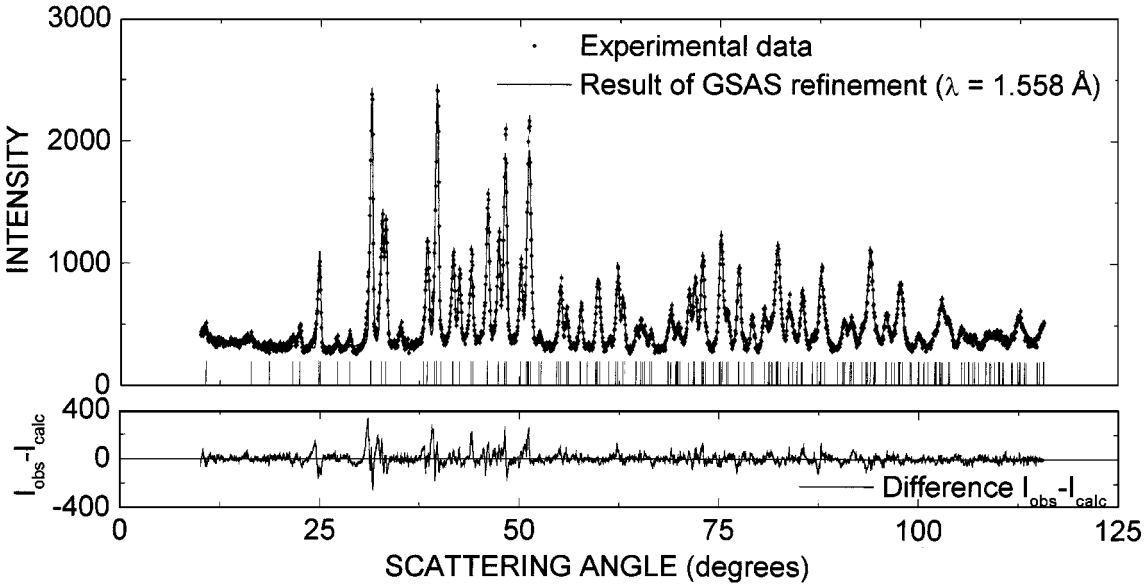

FIG. 2. Observed (crosses), calculated (continuous line), and difference (bottom) powder diffraction profiles of $La_5Si_2BO_{13}$. The positions of Bragg peaks are indicated as vertical ticks.

(6–9) to assess the effect of changing cation size and charge due to crystal chemical substitutions of $La_5Si_2BO_{13}$ apatite.

Nontetrahedral Polyhedra M1

Nontetrahedral cations in $P6_3/m$ apatites are structurally present in two sites (Fig. 3). One is the La1 or in general $M1$ site, which is ninefold coordinated by three symmetry equivalent groups of three oxygens, and the other one is an irregular sevenfold coordinated polyhedron (La2 or in general $M2$). The latter polyhedron comprises the column anion as well (here an oxygen (O4), more frequently OH, Cl, F); this site is generally named X site (6), since it lies on the sixfold axis. The O4 is the only oxygen not linked in the Si,B tetrahedron, while the other O1, O2, and O3 oxygens are at tetrahedral vertices.

In Fig. 4 the average $M1$–O bond lengths are shown for (Ca, Sr, Ba, Pb)$_5$(PO$_4$)$_3$(OH, Cl, F) apatites vs ionic radius (10). The observed trend indicates that the polyhedral average bond lengths are dictated mainly by changes in the ionic radius, and they are almost unaffected by the column anion. The $La_5Si_2BO_{13}$ value falls slightly above the trend in Fig. 4. A slight increase in average $M1$–O distance is in fact observed as an effect of the increase in size of the tetrahedral polyhedron (see following section).

The $M1$ polyhedron for $La_5Si_2BO_{13}$ is, however, more regular then in Ca-bearing apatites, as it can be shown by the difference between the shorter and the longer $M1$–O distances (Fig. 5). This difference, which may be considered an index of the polyhedral distortion, decreases with increasing cation size for (Ca, Sr, Ba, Pb)$_5$(PO$_4$)$_3$(OH, Cl, F)

TABLE 2
Atomic Fractional Coordinates and Isotropic Displacement Factors (10^{-2} Å) of $La_5Si_2BO_{13}$

	Site	x	Y	z	U_{iso}
La1	4*f*	0.33	0.66	− 0.0008(5)	2.03(8)
La2	6*h*	0.2330(4)	− 0.0153(4)	0.25	1.31(7)
$Si_{0.66}B_{0.33}$	6*h*	0.4036(5)	0.3741(5)	0.25	1.57(11)
O1	6*h*	0.3273(4)	0.4848(5)	0.25	1.07(10)
O2	6*h*	0.5952(5)	0.4683(5)	0.25	2.12(11)
O3	12*i*	0.3452(4)	0.2559(4)	0.0719(3)	1.95(7)
O4	2*a*	0	0	0.25	2.56(15)

TABLE 3
Individual and Average Interatomic Distances (Å) within Coordination Polyhedra of $La_5Si_2BO_{13}$

La1–O1	2.490(4) × 3	La2–O3	2.470(3) × 2
La1–O2	2.499(4) × 3	La2–O2	2.474(4)
La1–O3	2.825(3) × 3	La2–O3	2.596(4) × 2
Average (C.N. = 9)	2.605	La2–O1	2.695(5)
		La2–O4	2.304(3)
T–O1	1.557(5)	Average (C.N. = 7)	2.515
T–O2	1.586(5)		
T–O3	1.615(4) × 2		
Average (C.N. = 4)	1.593		

TABLE 4
Predicted and Calculated Bond Strengths (in Valence Units) for Atoms in $La_5Si_2BO_{13}$

	Predicted	Obtained
La1	3.0	3.02
La2	3.0	2.91
$Si_{0.66}B_{0.33}$	3.66	3.63
O1	− 2	− 2.09
O2	− 2	− 2.19
O3	− 2	− 1.79
O4	− 2	− 2.10

apatites. $La_5Si_2BO_{13}$ instead has a significantly lower distortion and it is clearly off the ionic trend. A very low distortion is also present in the vacancy bearing $La_{4.67}Si_2O_{13}$ apatite (*M*1–O3 minus *M*1–O1 is 0.303 Å). This effect is not due to the larger size of the tetrahedral polyhedron in $La_5Si_2BO_{13}$ with respect to the PO_4-bearing apatites: comparison with Ca apatites with As in the tetrahedral site (11) suggests that increasing the size of the tetrahedral cation increases the distortion in the *M*1 polyhedron (0.43 vs 0.39 Å in $Ca_5(AsO_4)Cl$ vs $Ca_5(PO_4)Cl$ apatites), indicating that the lower distortion in $La_5Si_2BO_{13}$ may be an effect of substitution with a trivalent cation.

Nontetrahedral Polyhedra M(2)

In the general apatite, the *M*2 site is coordinated by five oxygens, the column anion, and a seventh oxygen (O1) tied with a weaker bond. In $La_5Si_2BO_{13}$ all seven coordinating atoms are oxygens, because the column anion is itself oxygen (O4).

The most interesting structural feature in the M2 polyhedron is the extremely short M2–O4 bond length. In Fig. 6 the cation to anion distance for the *M*2–X is shown in

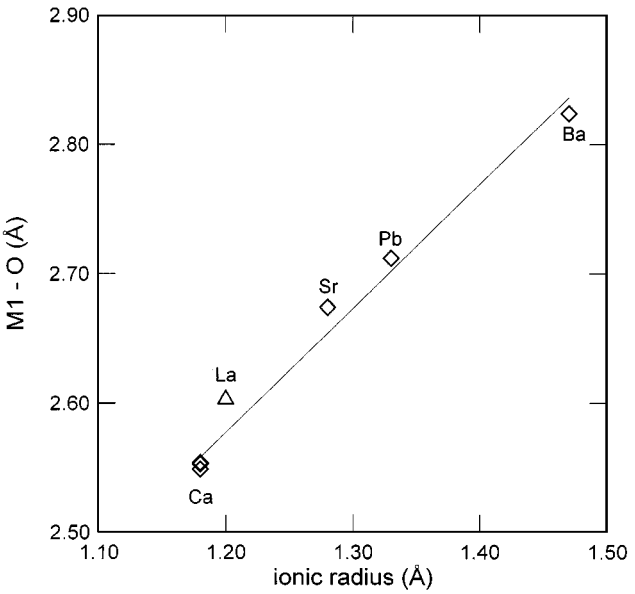

FIG. 4. Average *M*1–O distances vs cation ionic radius (ionic radii from (10)). The cation occupying the site is marked. Diamonds indicate samples with tetrahedral P; triangle indicates this work sample. Data are from Ref. (6) for $Ca_5(PO_4)_3(OH, Cl, F)$, Ref. (7) for $Sr_5(PO_4)_3OH$, Ref. (8) for $Ba_5(PO_4)_3Cl$, and Ref. (9) for $Pb_5(PO_4)_3Cl$ apatites.

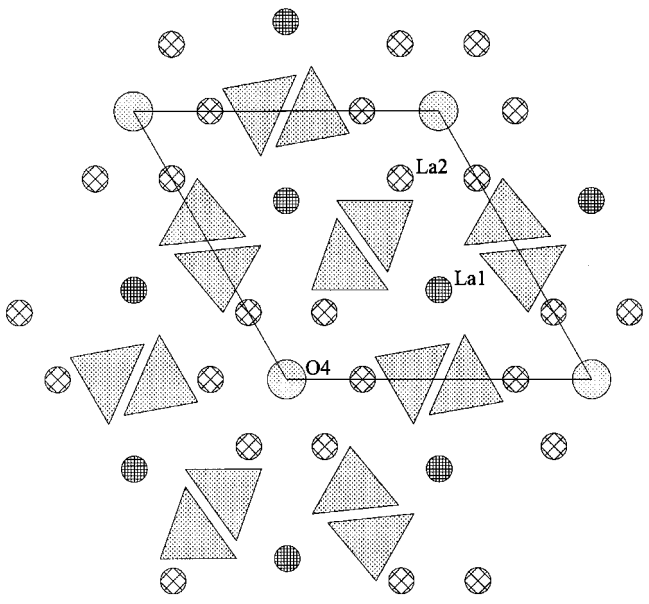

FIG. 3. The structure of $La_5Si_2BO_{13}$. View along the *c* axis.

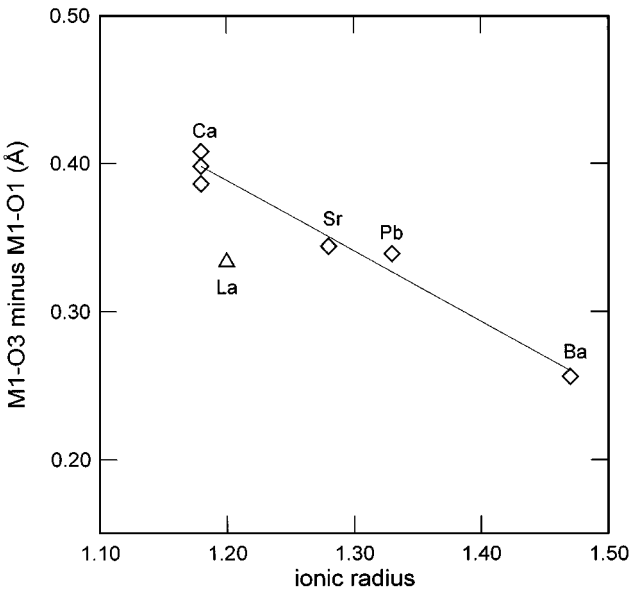

FIG. 5. Difference between the shorter and longer bond lengths in the *M*1 polyhedron vs ionic radius. Symbols are as in Fig. 4.

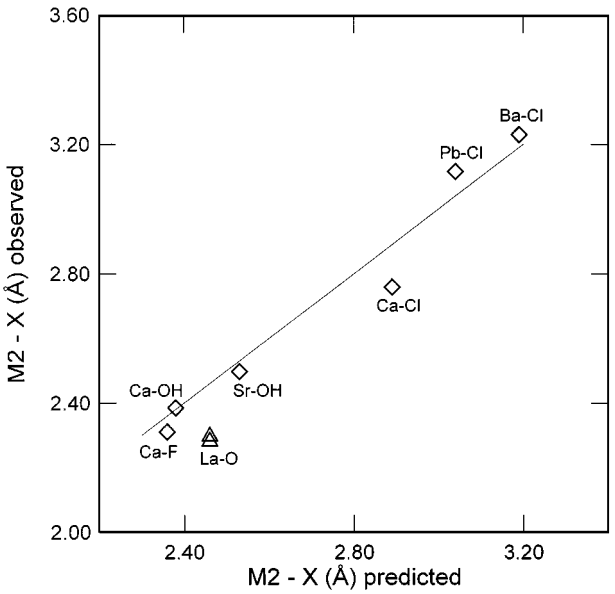

FIG. 6. Observed vs predicted by ionic radius sum of the *M2–X* distances. Cation–anion couples are indicated. Diamonds indicate samples with tetrahedral P; triangle indicates this work sample and sample from Ref. (5).

several (Ca, Sr, Ba, Pb)$_5$(PO$_4$)$_3$(OH, Cl, F) apatites, together with this work and $La_{4.67}Si_2O_{13}$ data. For comparison, we report the trend that would be present if the distance corresponded exactly to the sum of the cation and anion radii. It appears that (Ca, Sr, Ba, Pb)$_5$(PO$_4$)$_3$(OH, Cl, F) apatites almost follow the above trend, while in $La_5Si_2BO_{13}$ and $La_{4.67}Si_2O_{13}$ this distance is significantly lower. This extreme bond shortening can be explained by bond valence requirements. The column oxygen is coordinated only by three La2 cations; if no correction for bond length is taken into account, the column oxygen would receive three of seven valence units from each La2 and would be as a whole highly underbonded (1.28 valence units). Charge balance is obtained by a strong approach of La2 to the column oxygen. It must be stressed that the isotropic displacement parameter for O4 is very high, the highest of the refined sites, suggesting that some positional disorder may be present. Anisotropic refinement of the O4 atomic position showed significant elongation along the *c* axis. However a refinement splitting the position of the O4 site could not be performed owing to the low contribution of the O4 site, in 2*a* position, to the overall scattering.

Si, B tetrahedron

Both Si and B are located on the tetrahedral site in this work's apatite. Several atempts to locate B in triangular coordination did in fact result in negative displacement factors or poorer agreement in the refinement factors. The tetrahedral size can be easily related in apatites to the size of the cation present in it. In $La_5Si_2BO_{13}$ the substitution of B for Si gives rise to a tetrahedron whose average bond length is exactly of the size predicted by the averaged sum of cation and anion ionic radii (1.59 Å). It was also observed (6) that increasing the size of the tetrahedral cation slightly increases the M1–O distances, while the tetrahedron is not affected by the cation in *M*1.

CONCLUSIONS

The first structural determination of an apatite homolog fully occupied by trivalent lanthanide ions has been carried out. Structural relationships with other members of this family are discussed. La-deficient or in general Rare Earth-deficient Si apatites can be considered to derive from this archeotype compound.

REFERENCES

1. D. Mazza and S. Ronchetti, *Mater Res. Bull.* **34**(9), 1375–1382 (1999).
2. S. Nakayama and M. Sakamoto, *J. Eur. Ceram. Soc.* **18,** 1413–1418 (1998).
3. A. C. Larson and R. B. Von Dreele, GSAS: General Software Analysis System manual, Los Alamos National Laboratory Report, LAUR 86–748, 1994.
4. E. A. Kuz'min and A. N. V. Belov, *Dok. Akad. Nauk SSSR, DANKA* **165,** 88–90 (1965).
5. I. D. Brown and D. Altermatt, *Acta Crystallogr.* **41,** 244–247 (1985)
6. J. M. Hughes, M. Cameron, and K. D. Crowley, *Am. Mineral.* **74,** 870–876 (1989).
7. K. Sudarsanan and R. A Young, *Acta Crystallogr. B* **28,** 3668–3670 (1972).
8. M. Hata, F. Marumo, and S. I. Iwai, *Acta Crystallogr. B* **35,** 2382–2384 (1979).
9. Y. Dai and J. M. Hughes, *Can. Mineral.* **27,** 189–192 (1989).
10. R. D. Shannon and C. T Prewitt, *Acta Crystallogr. B* **25,** 925–945 (1969).
11. T. A. Wardojo and S.-J. Hwu, *Acta Crystallogr. C* **52,** 2959–2960 (1996).